



## CHAOTIC DYNAMICS OF A SPATIO-INHOMOGENEOUS MEDIUM

V. S. ANISHCHENKO, T. E. VADIVASOVA, G. A. OKROKVERTSKHOV,  
A. A. AKOPOV and G. I. STRELKOVA

*Institute of Nonlinear Dynamics, Physics Department,  
Saratov State University, 83, Astrakhanskaya Street,  
Saratov 410026, Russia*

Received December 15, 2004; Revised January 23, 2005

In the present paper we show that inhomogeneity of a continuous self-sustained oscillating medium can be a reason for the onset of chaotic behavior. It has been established that temporal chaotic dynamics typically arises in the medium with a linear mismatch of the natural frequency along a spatial coordinate, whereas a chaotic regime is not characteristic for the medium with randomly distributed frequencies. The interconnection has been revealed between the temporal chaotic behavior and the spatial formation of imperfect clusters. The spectral and correlation analysis as well as the linear analysis of stability of regular and chaotic regimes in the inhomogeneous medium are performed. The correlation of the instantaneous phase dynamics of oscillations with the behavior of autocorrelation functions has been examined. It has been established that the characteristics of temporal chaos correspond to a spiral attractor (Shilnikov's attractor).

*Keywords:* Inhomogeneous medium; partial synchronization; mean frequency; clusters; temporal chaotic dynamics.

### 1. Introduction

Over a long period of time, distributed systems and media have been the subject of constant interest of investigators in the field of nonlinear dynamics. The problem of deterministic chaos appeared and developed in a close connection with the theory of turbulence in continuous media [Ruelle & Takens, 1971; Swinney *et al.*, 1977; Golub & Benson, 1980]. Chaotic dynamics is typical of a wide class of nonlinear distributed systems and media and was widely covered in the scientific literature. For example, it is well known that temporal chaotic turbulent regimes can be observed in the Ginzburg–Landau classical model of a self-sustained oscillatory medium [Sakaguchi, 1990; Shraiman *et al.*, 1992; Chaté, 1994]. A large number of freedom degrees and the variety of nonlinear effects realized in distributed systems enable one to expect the appearance of new scenarios of chaos development as well as new types

of chaotic attractors as compared with lumped systems. Nevertheless, as numerous numeric and experimental studies have shown, the dimension of chaotic attractors of distributed systems appears to be, as a rule, not large, and essential differences are not revealed between temporal chaotic oscillations of low-dimensional systems and of systems with high (or infinite) dimension [Brandstater *et al.*, 1983; Malreison *et al.*, 1983; Anishchenko *et al.*, 1986]. Thus, chaotic regimes in distributed systems and media can be classified by using the notions of chaotic attractors in low-dimensional systems [Shilnikov & Afraimovich, 1983; Shilnikov, 1997; Anishchenko, 1995] and by selecting attractors of a saddle-focus type (Shilnikov's attractors), that appear via a quasiperiodic regime destruction (torus-attractors), switching-type attractors and others.

A topical problem relating to distributed systems and media is the influence of spatial

inhomogeneity, i.e. the dependence of system parameters on spatial coordinates, on a dynamical regime of a system. This subject is especially important since the inhomogeneity is inevitably present in any real distributed system and may essentially affect its behavior. In the case of self-sustained oscillatory systems and media the inhomogeneity may lead to a natural frequency mismatch of different elements of the system. When varying the parameter that controls the interaction between elements, partial or global synchronization can be observed [Sakaguchi *et al.*, 1978; Winfree, 1980; Kuramoto, 1984; Yamaguchi & Shimizu, 1984; Strogatz & Mirollo, 1988; Afraimovich *et al.*, 1995]. Partial synchronization regimes corresponding to frequency cluster formation have been revealed and examined in a number of papers where chains of self-sustained oscillators with a linear and random frequency gradient were considered [Ermentrout & Kopell, 1984; Osipov *et al.*, 1997; Osipov & Sushchik, 1998]. Such models can be used to describe phenomena which are observed in living tissues and distributed chemical reactions [Winfree, 1980; Diamant *et al.*, 1970; Sarna *et al.*, 1972; Linkens & Satardina, 1977] as well as in hydrodynamics [Noak *et al.*, 1991]. Similar cluster regimes can also be registered in numeric simulation of a continuous self-sustained oscillatory system described by the Ginzburg–Landau equation with a real diffusion coefficient and a linear gradient of natural frequencies [Ermentrout & Troy, 1986]. Nevertheless, the major results concerning frequency clusters have been obtained only for systems with a discrete spatial coordinate (of chains). In the paper [Osipov & Sushchik, 1998] it was noted that in some cases a nonregular temporal dynamics can be found in a chain with a linear gradient of frequencies. However, the characteristics of the nonregular regime have not been studied. The appearance of nonregular temporal oscillations in a distributed medium, that is caused by the presence of spatial inhomogeneity, is a principally important effect deserving to be examined in more detail. In the present paper we study a continuous self-sustained oscillatory medium with two types of natural frequency mismatch, namely, with a linear gradient and a random one. The main objective of our work is to explore appearance conditions and fundamental properties and characteristics of nonregular self-sustained oscillations. In particular, a special attention is paid to the spectral and correlation analysis of oscillations and to the peculiarities of phase dynamics.

## 2. The Model of Medium under Study

We consider a one-dimensional self-sustained oscillating medium that is governed by the Ginzburg–Landau equation with real parameters and with the oscillation frequency depending on a spatial coordinate:

$$a_t = i\nu(x)a + \frac{1}{2}(1 - |a|^2)a + ga_{xx}, \quad (1)$$

where  $i = \sqrt{-1}$ ,  $a(x, t)$  is the complex amplitude of oscillations; independent variables  $t$  and  $x \in [0, l]$  are the time and the dimensionless spatial coordinate, respectively.  $a_t$  is the first time derivative, and  $a_{xx}$  is the second derivative with respect to the spatial coordinate. In numeric simulation the medium length is fixed as  $l = 50$ . The diffusion coefficient  $g$  is assumed to be the same in all points of the medium. For  $g \rightarrow 0$ , oscillations in various points of the medium possess different frequencies which are defined by a function  $\nu(x)$ . We study two types of the spatial mismatch  $\nu(x)$ , namely, linear and random ones. The linear mismatch is defined as follows:

$$\nu(x) = x \frac{\Delta}{l}, \quad (2)$$

where  $\Delta$  is the maximal mismatch, i.e. the mismatch between boundary points of the medium. The model of the medium Eq. (1) with the linear mismatch can be treated as a limiting case of an inhomogeneous chain of quasi-harmonic self-sustained oscillators [Osipov & Sushchik, 1998; Vadivasova *et al.*, 2001] when passing to a continuous spatial coordinate. A similar model of the medium has been examined in [Ermentrout & Troy, 1986]. In the case of random mismatch the function  $\nu(x)$  is defined as follows. First, we find a realization of a random function  $y(x)$  that is given by the following stochastic differential equation (SDE):

$$\frac{dy}{dx} = -\alpha y + \sqrt{2D}\xi(x). \quad (3)$$

$x$  is the independent variable, and  $\xi(x)$  is the normalized Gaussian white noise source,  $D$  is the noise intensity, and  $\alpha$  is the parameter controlling the spatial correlation and the variance of random quantities  $y(x)$ . The initial condition  $y(0)$ , step  $h_x$  and the initializing variable of a random number source are chosen to be the same in all numeric calculations. The autocorrelation function (ACF) of

the random function  $y(x)$  reads

$$\psi_y(s) = \frac{D}{\alpha} \exp(-\alpha|s|), \quad s = x_2 - x_1. \quad (4)$$

Then, using the obtained function  $y(x)$  we can write down the dependence  $\nu(x) \in [0, \Delta]$  as follows:

$$\nu(x) = \Delta \frac{y(x) - y_{\min}}{y_{\max} - y_{\min}}, \quad (5)$$

where  $y_{\min}$  and  $y_{\max}$  are minimal and maximal values of the random variable  $y$  for the given realization of the random function on the interval  $[0, l]$ ;  $\Delta$  is the maximal frequency mismatch between the medium elements for  $g = 0$ .

The boundary conditions for Eq. (1) are set in the form  $a_x(x, t)|_{x=0, l} \equiv 0$ . The initial condition of the medium is chosen randomly near some homogeneous distribution  $a_0 = \text{const}$ . Equation (1) is integrated numerically by means of the finite difference method according to an implicit scheme with forward and backward sweeps. We calculate the real and imaginary components of the complex amplitude  $a(x, t)$

$$a_1(x, t) = \text{Re } a(x, t), \quad a_2(x, t) = \text{Im } a(x, t), \quad (6)$$

and the real amplitude  $A(x, t)$  and the phase  $\phi(x, t)$  of oscillations

$$\begin{aligned} A(x, t) &= |a(x, t)| = \sqrt{a_1^2 + a_2^2} \\ \phi(x, t) &= \arg a(x, t) \\ &= \arctg \frac{a_2}{a_1} \pm \pi k, \quad k = 0, 1, 2, \dots \end{aligned}$$

Since the phase changes continuously with time, we add the term  $\pm \pi k$  to the expression for the phase. The average frequency of oscillations in a medium point with coordinate  $x$  is estimated by the formula:

$$\Omega(x) = \langle \phi_t(x, t) \rangle = \lim_{T \rightarrow \infty} \frac{\phi(x, t_0 + T) - \phi(x, t_0)}{T}. \quad (7)$$

The angle brackets mean time averaging.

### 3. Cluster Synchronization and Chaos in the Medium with Linear Inhomogeneity

Without mismatch,  $\Delta = 0$ , the medium Eq. (1) can demonstrate a homogeneous stationary regime only, i.e.  $a(x, t) \equiv a_0$ . When the frequency mismatch is introduced, the average oscillation frequency  $\Omega$  changes along the spatial coordinate  $x$ . In the case of linear mismatch [Eq. (2)] and for the

given parameter  $\Delta$  the formation of frequency synchronization clusters can be observed in a certain region of diffusion coefficient values. Depending on chosen parameters, one can get perfect and imperfect clusters. In the regime of perfect clusters, the medium is divided into  $M$  clusters (regions), each demonstrating strongly identical average oscillation frequency  $\Omega_i$ , where  $i = 1, 2, \dots, M$  is the cluster number. In the regime of imperfect clusters the average frequency continuously depends on the spatial coordinate. In this case the clusters are identified as space regions (areas) for which the average oscillation frequencies are close to each other (slanting parts of the  $\Omega(x)$  dependence). Besides, the medium also includes intercluster regions that correspond to fast changes of the average frequency in space. Similar clusters have been observed earlier in a chain of dissipatively coupled self-sustained oscillators [Osipov & Sushchik, 1998]. However, in this case the average frequency in the regime of imperfect clusters cannot change continuously along the chain since the spatial coordinate is discrete.

Our studies of the medium Eq. (1) have shown that the character of temporal behavior of the system depends on the form of frequency clusters. For the perfect cluster regime, the oscillations are regular (periodic or quasi-periodic ones). In the case of imperfect clusters the medium demonstrates a nonregular temporal behavior resembling chaotic dynamics. Figure 1 exemplifies perfect and imperfect frequency clusters in the medium Eq. (1) with the linear frequency gradient. The same figure also shows the corresponding diagrams reflecting the spatio-temporal dynamics of the real amplitude  $A(x, t)$ . There is no point in speaking about spatial order or disorder in the system being studied as the system length includes only two or three spatial oscillations for the chosen values of the parameters  $g$  and  $\Omega$ . We cannot respectively judge about turbulence since the latter notion implies a nonregular behavior of the medium both in time and in space. However, as the system length  $l$  increases or the parameter  $g$  decreases, the medium with imperfect clusters can also exhibit a spatial disorder.

Cluster structures characterize a spatial distribution of the average oscillation frequency of the medium Eq. (1). The relation between this quantity and characteristic frequencies being present in the power spectrum of oscillations is not entirely obvious. From a viewpoint of the power spectrum, the real existence of frequency clusters can be demonstrated by constructing spatio-spectral diagrams

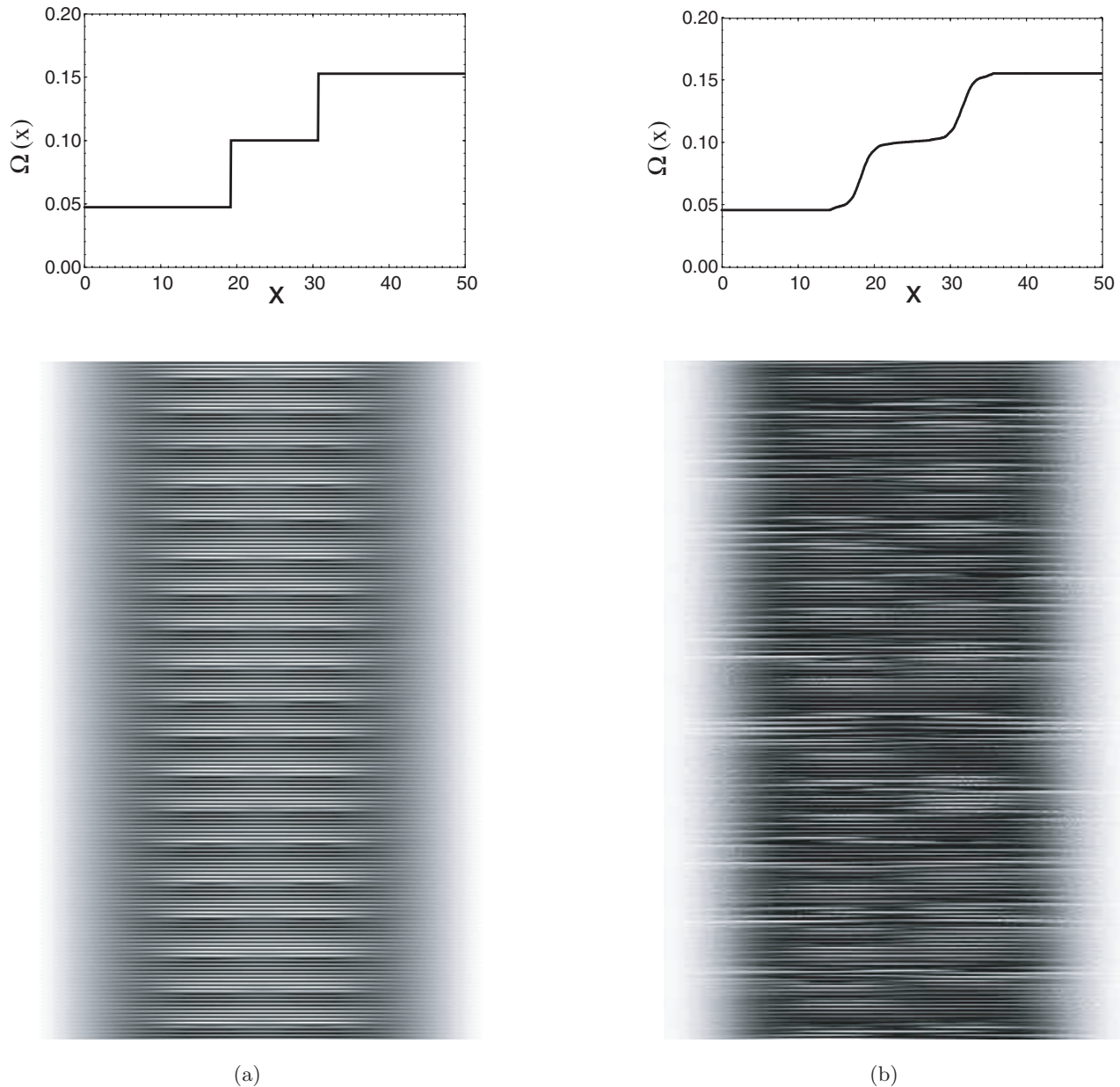


Fig. 1. Medium behavior in the regime of cluster synchronization. (a) Perfect cluster (upper row) and the corresponding spatio-temporal diagram for  $g = 1.0$ ; (b) imperfect clusters and the spatio-temporal diagram for  $g = 0.85$ . The grey color gradient in the spatio-temporal diagrams (low row) reflects real amplitude values  $A(x, t)$ . The white color corresponds to the maximal value of the amplitude and the black one to the minimal value. The horizontal axis is  $x$  coordinate values and the vertical one is time. The calculations are performed with discretization steps  $h_t = 0.01$  and  $h_x = 0.001$ .

that are shown in Fig. 2 and reflect the distribution of power over frequencies as a function of the spatial coordinate. A definite structure can be well distinguished in the diagrams. The distribution of the spectral maximum repeats the distribution of the average frequency  $\Omega(x)$ . In the regime of perfect clusters, the average frequency completely matches the frequency of the spectral maximum [Fig. 2(a)].

The boundary between clusters coincides with the redistribution of powers between neighboring spectral lines. In the regime of imperfect clusters, agreement between the frequencies is approximate and is essentially violated in intercluster regions. Besides, as can be seen from Fig. 2(b), the oscillations in the imperfect cluster regime are characterized by a more complicated power spectrum distribution that

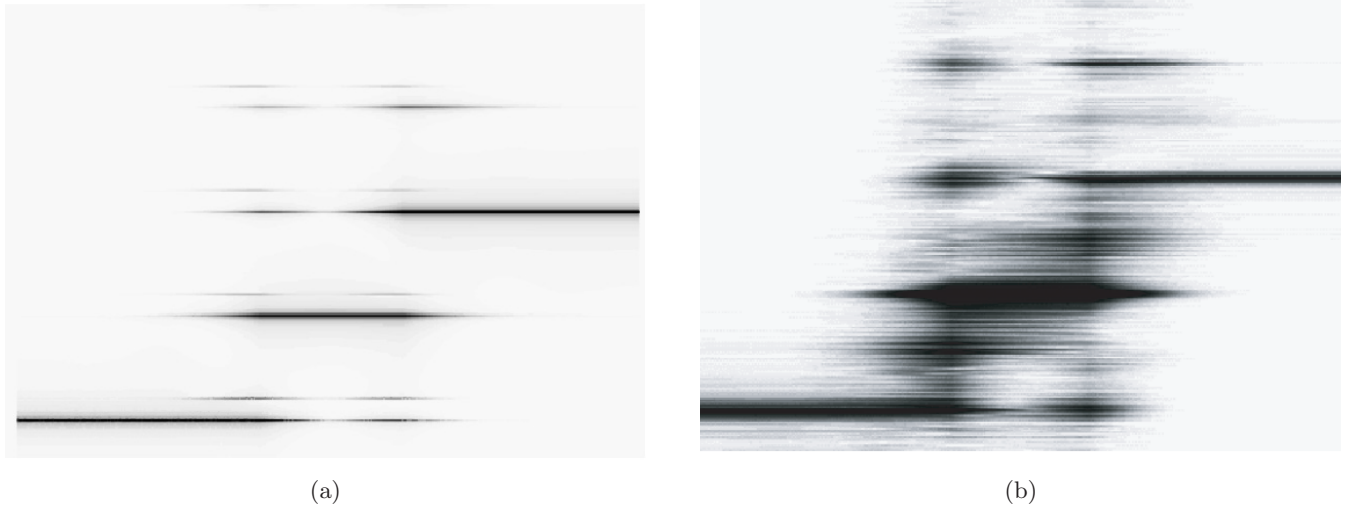


Fig. 2. Spatio-frequency diagrams of  $a_1(x, t)$  oscillations for (a)  $g = 1.0$  (regime of perfect clusters of the average frequency) and (b)  $g = 0.85$  (regime of imperfect clusters). The grey color gradient denotes different values of the power spectrum density  $S(x, \omega)$  in a linear scale. The white color corresponds to zero value of  $S(x, \omega)$  and the black one to its maximal value. The horizontal axis is  $x$  coordinate values and the vertical one is the frequency.

is related with their nonregular character. Harmonics and combination frequencies are especially well pronounced in intercluster regions.

Consider in detail the basic characteristics of medium oscillations in some spatial points for the case of perfect and imperfect cluster formation. For fixed points  $x = x_1$  we construct phase projections of oscillations on the plane  $(a_1, a_2)$ , spectral power densities and temporal autocorrelation functions. The ACF and power spectra are calculated using independent methods. Under the assumption that oscillations are ergodic and stationary, the ACF of the process  $a_1(x, t)$  is computed directly from its definition:

$$\psi_{a_1}(x, \tau) = \langle a_1(x, t)a_1(x, t + \tau) \rangle - \langle a_1(x, t) \rangle^2, \quad (8)$$

where the angle brackets mean time averaging. Then the ACF is normalized on its maximal value, i.e.  $\Psi_{a_1}(x, \tau) = \psi_{a_1}(x, \tau)/\psi_{a_1}(x, 0)$ .

Characteristics of oscillations in the regime of three perfect clusters are shown in Fig. 3 for  $g = 1.0$  and in the spatial point  $x_1 = 25$  (the second cluster center). The phase portrait projection pictured in Fig. 3(a) indicates a quasi-periodic character of oscillations. Figure 3(b) illustrates the normalized power spectrum of oscillations  $a_1(x_1, t)$ . The frequency of the basic spectral maximum, that corresponds to the largest power density, coincides

with the average frequency in the considered spatial point, i.e. with the frequency of the second cluster  $\Omega_2 = 0.1 \pm 10^{-4}$ . Besides, the spectrum exhibits peaks at the frequency of the first cluster  $\Omega_1 = 0.0472 \pm 10^{-4}$  that is incommensurable with  $\Omega_2$ , at the frequency of the third cluster  $\Omega_3 = 0.1527 \pm 10^{-4} = 2\Omega_2 - \Omega_1$ , and at some combination frequencies. The real amplitude  $A(x_1, t)$  represents an envelope of the oscillations  $a_1(x_1, t)$ . Respectively, the power spectrum of  $A(x_1, t)$  that is shown in Fig. 3(c) demonstrates peaks at the difference frequency  $\Omega_2 - \Omega_1$  and its harmonics. The ACF of the process  $a_1(x_1, t)$  is presented in Fig. 3(d) and corresponds to a quasi-periodic regime.

Figure 4 illustrates oscillations at the point corresponding to the second cluster center ( $x_1 = 25$ ) but now in the regime of imperfect clusters for  $g = 0.85$ . The projection of oscillations on the plane  $(a_1, a_2)$  is shown in Fig. 4(a) and indicates a more complicated temporal behavior of the medium. The power spectrum of the process  $a_1(x_1, t)$  is continuous [Fig. 4(b)], although several peaks at characteristic frequencies can be distinguished. The frequency of the basic spectral maximum  $\omega_{\max} = 0.1 \pm 10^{-4}$  coincides, within the calculation accuracy, with the average frequency  $\Omega(x_1)$ . As before, we can denote it as the frequency of the second cluster  $\Omega_2$ , although, strictly speaking, the average frequency is not strongly the same at all points of

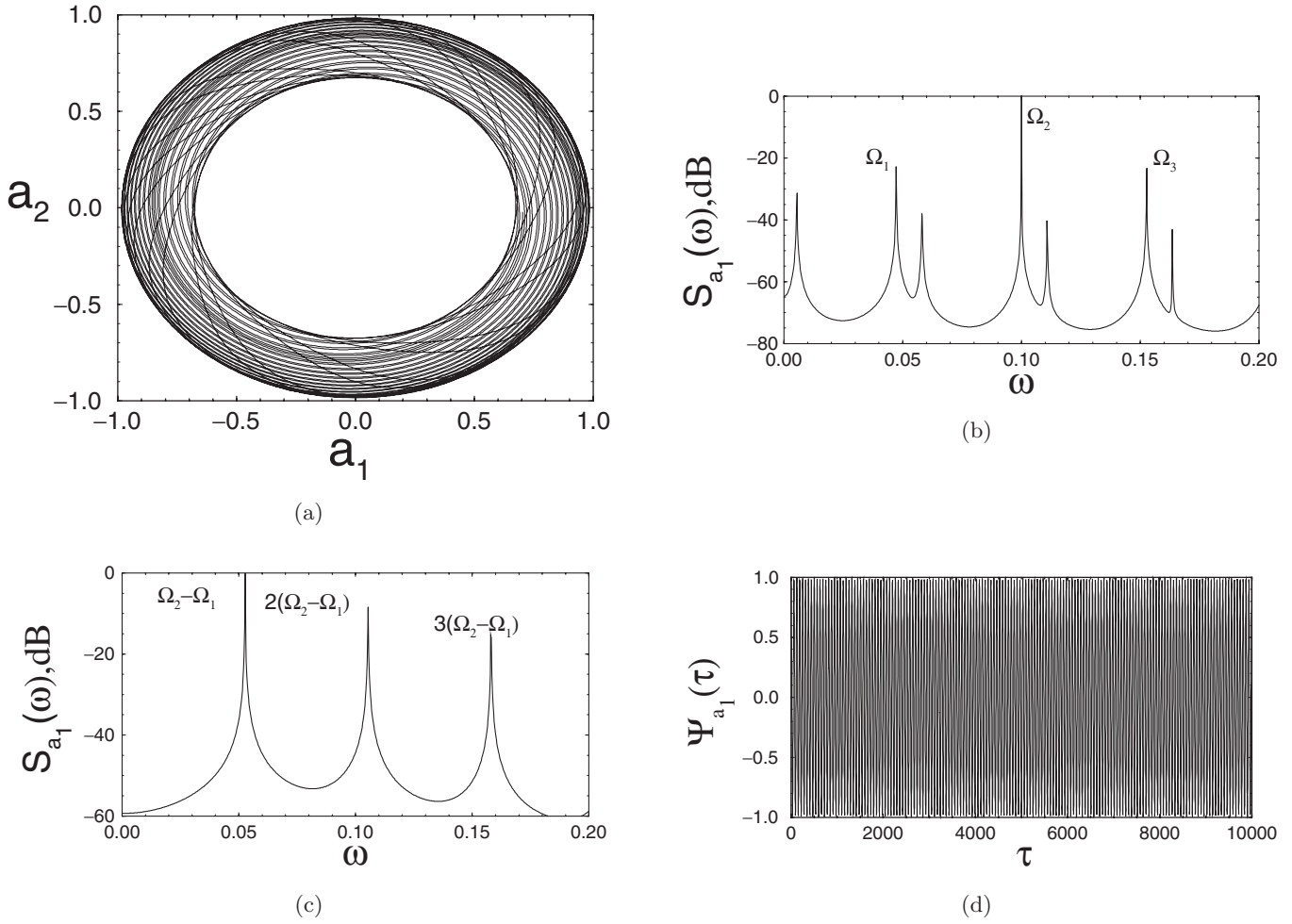


Fig. 3. Characteristics of oscillations at the point  $x_1 = 25$  (the cluster center) in the regime of perfect clusters for  $g = 1.0$ . (a) Phase portrait projection on the plane  $(a_1, a_2)$ ; (b) normalized power spectrum density of  $a_1(x_1, t)$  oscillations; (c) normalized power spectrum density of  $A(x_1, t)$  oscillations; and (d) normalized ACF of  $a_1(x_1, t)$ .

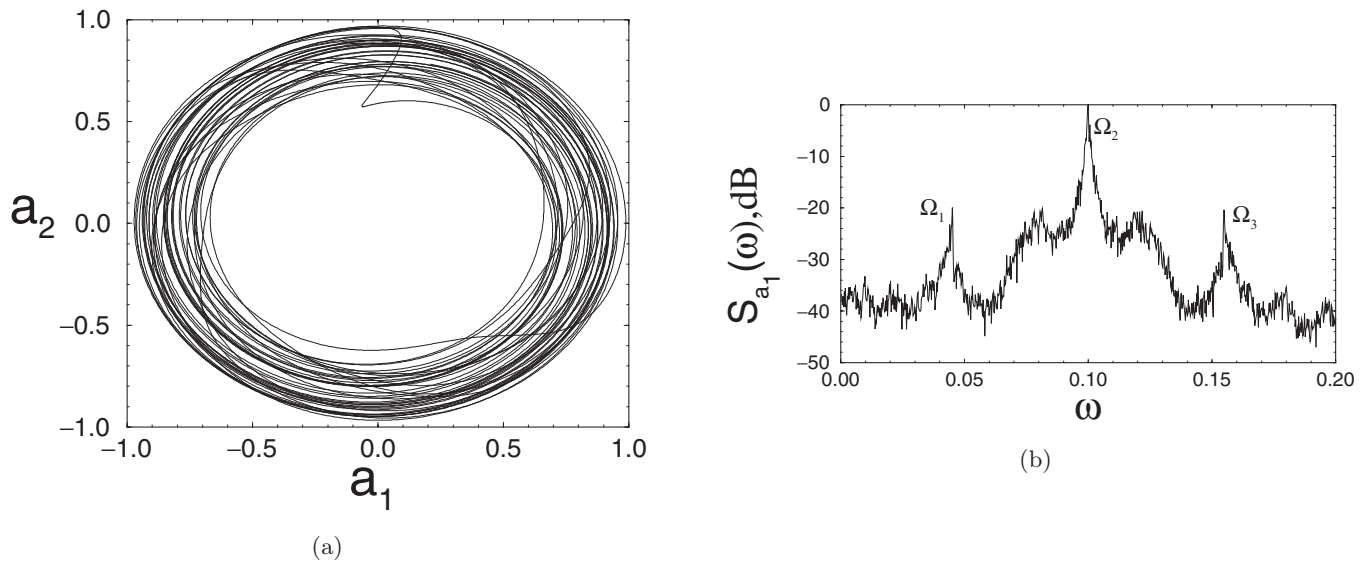


Fig. 4. Characteristics of oscillations at the point  $x_1 = 25$  (the cluster center) in the regime of imperfect clusters for  $g = 0.85$ . (a) Phase portrait projection on the plane  $(a_1, a_2)$ ; (b) normalized power spectrum density of  $a_1(x_1, t)$  oscillations; (c) normalized power spectrum density of  $A(x_1, t)$  oscillations; and (d) normalized ACF of  $a_1(x_1, t)$ .

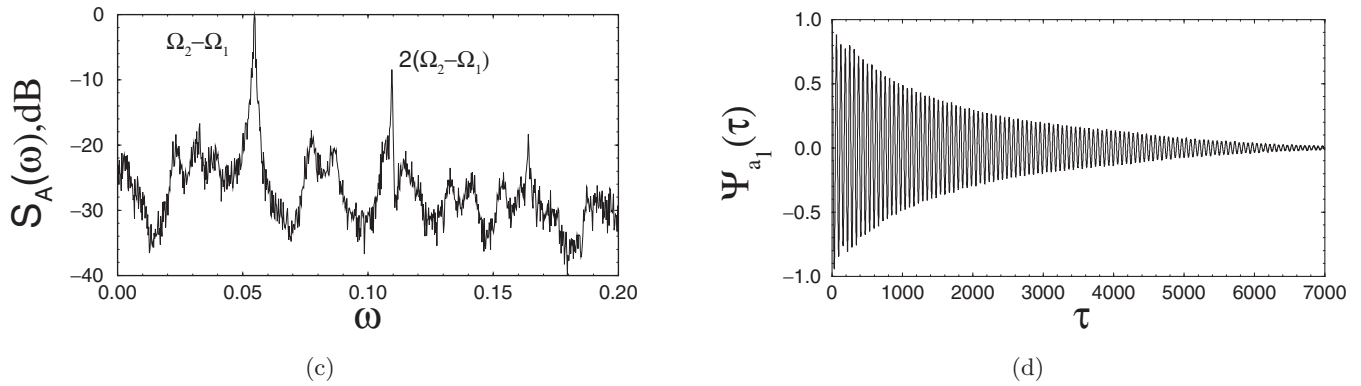


Fig. 4. (Continued)

the imperfect cluster. The spectrum also exhibits peaks at frequencies  $\Omega_1 = 0.0451 \pm 10^{-4}$  and  $\Omega_3 = 0.1548 \pm 10^{-4}$  that correspond to average frequency values in the center of the first and third

clusters. The continuous spectrum of the process  $A(x_1, t)$  is presented in Fig. 4(c) where  $\tilde{A}(x, t)$  is a centered process, i.e.  $\tilde{A}(x, t) = A(x, t) - \langle A(x, t) \rangle$  and  $\langle \dots \rangle$  denote the mean value. Here, one can see

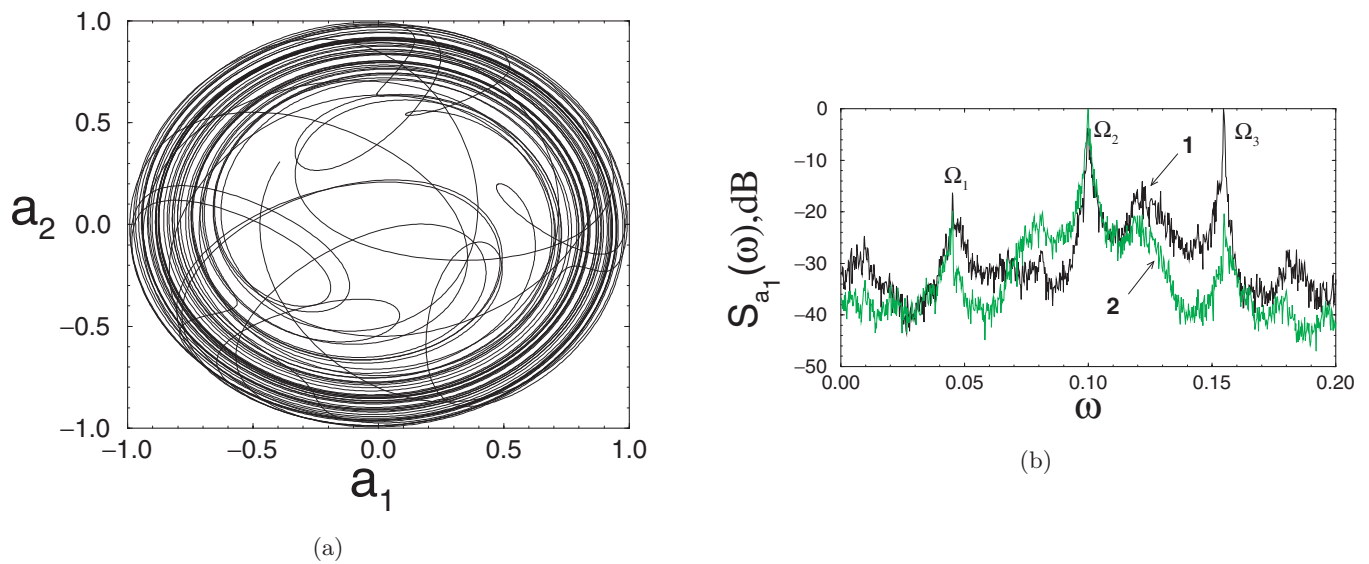


Fig. 5. Characteristics of oscillations at the point  $x_2 = 32$  (the cluster center) in the regime of imperfect clusters for  $g = 0.85$ . (a) Phase portrait projection on the plane  $(a_1, a_2)$ ; (b) normalized power spectrum density of  $a_1(x_2, t)$  oscillations, and (c) normalized ACF of  $a_1(x_2, t)$ .

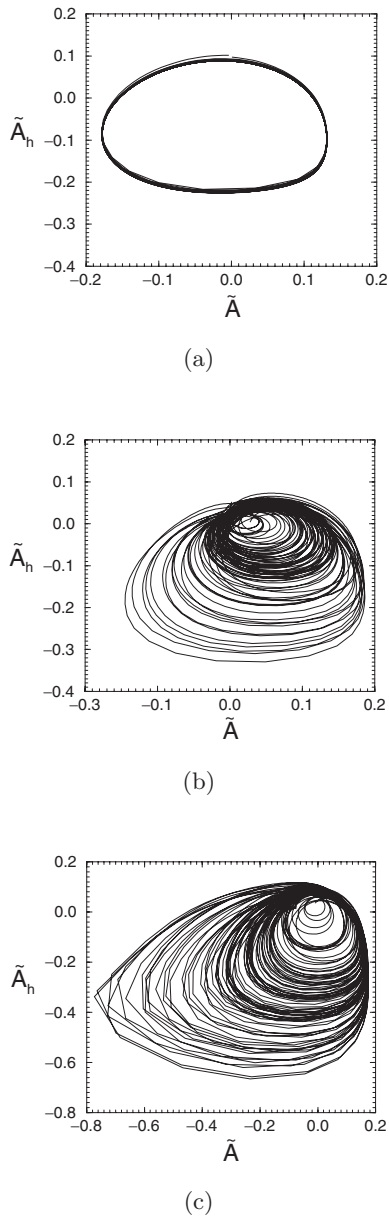


Fig. 6. Projections of oscillations on the plane  $(\tilde{A}(x_1, t), \tilde{A}_h(x_1, t))$  (a) in the regime of perfect clusters for  $g = 1.0$  and at the point  $x_1 = 25$ , (b) in the regime of imperfect clusters for  $g = 0.85$  and at the point  $x_1 = 25$  (the cluster center), and (c) in the regime of imperfect clusters for  $g = 0.85$  and at the point  $x_1 = 32$  (intercluster region).

peaks at the difference frequency  $\Omega_2 - \Omega_1$  and its harmonics. The decay of the ACF for  $a_1(x_1, t)$  [Fig. 4(d)] indicates the presence of mixing that in a deterministic system can be connected only with chaotic dynamics. It is worth noting that the ACF envelope decays almost exponentially.

In the same regime at  $g = 0.85$ , oscillations at the spatial point  $x_2 = 32$  corresponding to the intercluster region (between the second and third clusters) are much more complicated. As can be

seen from Fig. 5(a), the trajectory performs numerous disordered loops in the  $(a_1, a_2)$  projection. In Fig. 5(b) we compare two power spectra of oscillations  $a_1(x, t)$ , calculated at points  $x_2 = 32$  and  $x_1 = 25$  [the latter being analogous to Fig. 4(b)]. It is seen that the spectrum is rebuilding along the spatial coordinate. Since the point  $x_2$  is placed closer to the third cluster than to the second one, the basic spectral maximum at this point corresponds to the frequency  $\Omega_3$  (curve 1) rather than to  $\Omega_2$ , as at the point  $x_1$  (curve 2). It is important to emphasize that since the point  $x_2$  belongs to the intercluster region, the average frequency  $\Omega(x_2) = 0.1327 \pm 10^{-4}$  is essentially different from the frequency of the basic spectral maximum  $\Omega(x_3)$ . The ACF of  $a_1(x_2, t)$  oscillations also decays but not exponentially now [Fig. 5(c)].

For better understanding of the character of oscillations it is useful to analyze the behavior of trajectories not only in the  $(a_1, a_2)$  plane but also to introduce in some way projections of oscillations  $\tilde{A}(x_1, t)$  at a fixed point  $x = x_1$ . Projections on the plane  $(\tilde{A}, \tilde{A}_t)$  appear to be insufficiently illustrative. Therefore, we consider oscillations on the plane of variables  $\tilde{A}(x_1, t), \tilde{A}_h(x_1, t)$ , where  $\tilde{A}_h(x_1, t)$  is the Hilbert conjugate process with  $A(x_1, t)$ :

$$\tilde{A}_h(x, t) = \frac{1}{\pi} \int_{-\infty}^{\infty} \frac{\tilde{A}(x, \tau)}{t - \tau} d\tau. \quad (9)$$

Figure 6 exemplifies projections in regimes of perfect and imperfect clusters. It can be seen that the

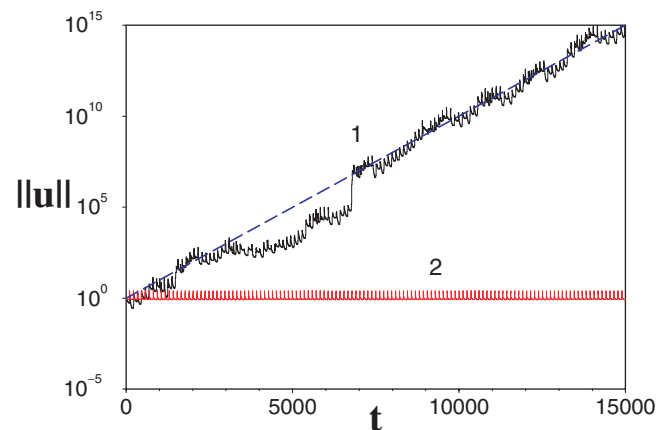


Fig. 7. Temporal dependence of the perturbation norm  $\|u(x, t)\|$  of oscillations in the medium Eq. (1) in the regime of imperfect frequency clusters for  $g = 0.85$  (curve 1) and in the regime of perfect clusters for  $g = 1.0$  (curve 2). Values of  $\|u(x, t)\|$  are given in a logarithmic scale. The dashed line denotes the exponential function  $\exp(\alpha t)$  with  $\alpha = \lambda_{\max} = 0.0023 \pm 10^{-4}$ .



periodic modulation corresponds to perfect clusters [Fig. 6(a)] whereas in the regime of imperfect clusters the obtained phase projections are very similar to phase projections of chaotic attractors of a saddle-focus type [Figs. 6(b) and 6(c)].

#### 4. Linear Analysis of Stability of Oscillations in Regimes of Perfect and Imperfect Cluster Synchronization

Since the considered model of the medium does not include noise sources, mixing can take place only due to the appearance of dynamical chaos, i.e. due to an absolute exponential instability of oscillations in the medium. To analyze the stability of oscillations, we integrate together with Eq. (1) a linearized equation for a small perturbation  $u(x, t)$  of the complex amplitude  $a(x, t)$ :

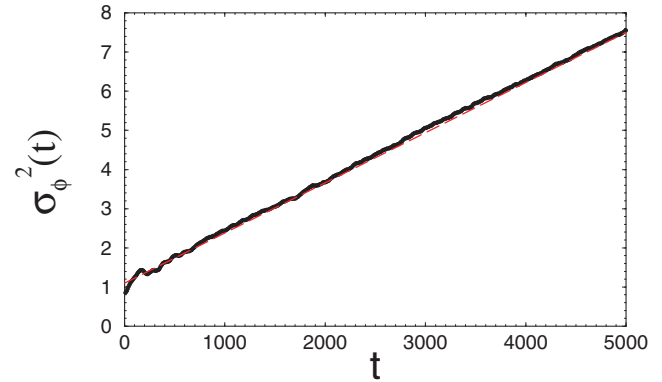
$$u_t = i\nu(x)u + \frac{1}{2}(1 - 2|a|^2)u - \frac{1}{2}a^2u^* + gu_{xx}, \quad (10)$$

where  $u^*$  is the complex conjugate quantity with  $u$ . Boundary conditions for the perturbation are set to be  $u_x(x, t)|_{x=0;l} \equiv 0$ . At every time moment  $t$  we consider an Euclidean norm of the perturbation  $\|u(x, t)\|$  that, taking into account the spatial coordinate discretization, can be reduced to a sum of a finite number of terms:

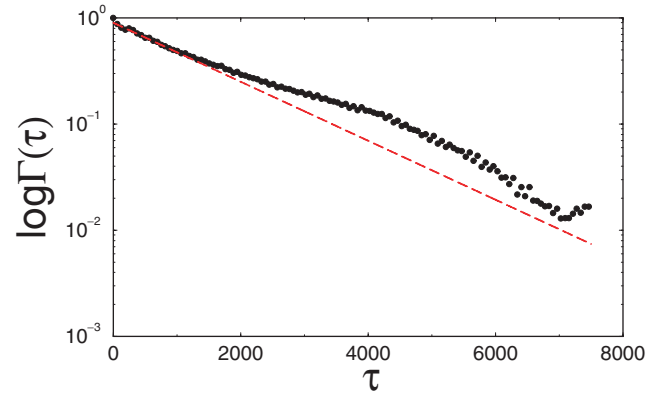
$$\begin{aligned} \|u(x, t)\| &= \left( \int_0^l ((\operatorname{Re} u(x, t))^2 + (\operatorname{Im} u(x, t))^2) dx \right)^{1/2} \\ &\approx \left( \sum_{k=1}^m (\operatorname{Re} u(x_k, t))^2 + (\operatorname{Im} u(x_k, t))^2 \right)^{1/2}, \end{aligned} \quad (11)$$

where  $m$  is the number of integration steps  $h_x$  along the system length. Our calculations have shown that in the regime of imperfect clusters the ACF decay is accompanied, on average, by an exponential increase of the perturbation norm in time (Fig. 7). The index of exponential increase  $\lambda_{\max}$  that is obtained for  $g = 0.85$  has the value  $\lambda_{\max} \approx 0.0023$ .

To check whether an oscillatory process in the medium is exponentially unstable in time, we calculate the maximal Lyapunov exponent  $\lambda_{\max}$  on a time series by using the algorithm proposed in [Wolf *et al.*, 1985]. The calculations give a positive value



(a)



(b)

Fig. 8. (a) Phase variance calculated for the regime of imperfect clusters ( $g = 0.85$ ) at the point  $x_1 = 25$  and its linear approximation (dashed line) corresponding to  $B_{\text{eff}} \approx 0.00064 \pm 10^{-5}$ . (b) ACF envelope of  $a_1(x_1, t)$  oscillations for  $g = 0.85$  and its approximation by  $\exp(-B_{\text{eff}}|\tau|)$  (dashed line), both shown in a linear-logarithmic scale.

of  $\lambda_{\max}$ , that is weakly dependent on the numerical scheme parameters. Results corresponding to different points of the medium appear to be slightly different but all of them preserve the same order of  $10^{-3}$ . For example, for optimal parameters of the numerical scheme the reconstruction method gives  $\lambda_{\max} = 0.002 \pm 0.0002$  for the point  $x_1 = 25$ , that is in good agreement with the Lyapunov exponent value obtained in the framework of the linear analysis of oscillation stability.

Hence, we can certainly state that the regime of imperfect frequency clusters arising in an inhomogeneous medium corresponds to a chaotic temporal behavior.

## 5. Mixing Rate and the Effective Phase Diffusion Coefficient of Chaotic Oscillations in the Regime of Imperfect Clusters

Anishchenko *et al.* [2003] and Anishchenko *et al.* [2004a] showed that for a wide class of chaotic self-sustained oscillating systems with lumped parameters, the rate of correlation splitting on large time intervals and the fundamental spectral line width are defined by the effective diffusion coefficient of an instantaneous phase of chaotic oscillations. With this, positive Lyapunov exponents (the Kolmogorov entropy) determine the rate of mixing in the transversal section of trajectories on an attractor. Mixing in the section takes place, as a rule, significantly faster than mixing along a flow of trajectories, that is related with the instantaneous phase dynamics. As seen from Fig. 4(d), the form of the ACF of the process  $a(x_1, t)$ , calculated for the regime of imperfect clusters, enables one to assume that the ACF envelope  $\Gamma_{a_1}(x_1, \tau)$  decays almost according to an exponential law. It is important to find out whether the rate of temporal correlation splitting in the inhomogeneous medium Eq. (1) is connected with the phase diffusion  $\phi(x, t) = \arg a(x, t)$ , as in finite-dimensional self-sustained oscillating systems in the regime of spiral chaos.

In our studies we consider a long realization of the process  $\phi(x, t)$  in the fixed point of the medium  $x = x_1$  and calculate the variance  $\sigma_\phi^2(x, t) = \langle \phi^2(x, t) \rangle - \langle \phi(x, t) \rangle^2$  on an ensemble of intervals of this realization (here the angular brackets mean ensemble averaging). The temporal dependence of the instantaneous phase variance obtained for the point  $x_1 = 25$  is presented in Fig. 8(a) for the regime of imperfect clusters. On the time interval  $t \in [0, 10000]$  the variance grows almost linearly. The angular coefficient of the variance growth can be found by means of a least-square method, and this estimation enables one to define the effective phase diffusion coefficient  $\phi(x, t)$ :

$$B_{\text{eff}} = \frac{1}{2} \left\langle \frac{d\sigma_\phi^2(x, t)}{dt} \right\rangle. \quad (12)$$

The angular brackets mean time averaging. The value of  $B_{\text{eff}}$  found at the point  $x_1 = 25$  coincides very well with the decrement of the ACF

decay of  $a_1(x_1, t)$  oscillations. The behavior of ACF envelope is compared with the exponential function  $\exp(-B_{\text{eff}}|\tau|)$  in Fig. 8(b). With this, the maximal Lyapunov exponent in the given regime exceeds the value of  $B_{\text{eff}}$  by order 1 and does not correspond to the rate of ACF decay. Thus, the ACF of chaotic oscillations of the medium Eq. (1) in the center of a frequency cluster decays almost exponentially with the decrement that is defined by the effective phase diffusion coefficient. Respectively, the width of the fundamental spectral line in the power spectrum must be also defined by  $B_{\text{eff}}$  since the spectral power density and the ACF are uniquely connected through the Wiener–Khinchin transformation. Apparently, spectral and correlation properties of chaotic oscillations in the cluster center can be qualitatively described by applying a model of harmonic noise, as done for the case of spiral chaos [Anishchenko *et al.*, 2003; Anishchenko *et al.*, 2004a]. The situation is quite different for the point  $x_2 = 32$  located in the intercluster region. As seen from Fig. 5(a), the oscillations  $a_1(x_2, t)$  are mostly nonregular. The temporal behavior of the phase is essentially nonmonotone.<sup>1</sup> The nonmonotone character of  $\phi(x_2, t)$  manifests itself in the fact that the average frequency  $\Omega(x_2)$  does not coincide with the maximal spectral peak frequency. In this case spectral and correlation characteristics of oscillations are not related directly with the temporal behavior of the phase [Anishchenko *et al.*, 2004b] and hence, the model of harmonic noise is not valid. Our calculations performed for the point  $x_2 = 32$  provide  $B_{\text{eff}} = 0.041 \pm 10^{-3}$ . However, this value is not at all related with the rate of the ACF decay of  $a_1(x_2, t)$  oscillations.

## 6. Cluster Synchronization and Chaos in the Medium with Random Inhomogeneity

Now we consider the case when the parameter  $\nu(x)$  in Eq. (1) is given by the expression Eq. (5) via the random function  $y(x)$  Eq. (3). Numerical calculations carried out for different values of the parameter  $\alpha$  that controls a spatial correlation of  $\nu(x)$  values and for different values of the diffusion coefficient  $g$  (for the fixed maximal mismatch  $\Delta = 0.2$ ) have revealed a number of peculiarities of the medium behavior in the presence of random

<sup>1</sup>The phase growth at the point  $x_1 = 25$  is not strongly monotonic too. However, its monotonicity is violated rarely, and these violations do not practically affect averaged characteristics.

frequency mismatch. For the same  $\Delta$ , the cluster synchronization in the medium with the random mismatch occurs in the region of much smaller values of the diffusion coefficient as compared with the case of linear mismatch. In other words, in this case one can much easily observe a global synchronization of the medium at the same frequency. Similar results were obtained for a chain of self-sustained oscillators in [Osipov & Sushchik, 1998]. For the random frequency mismatch a distribution of the average frequency  $\Omega(x)$  along a spatial coordinate typically corresponds to the perfect cluster formation. Figure 9 exemplifies the distribution of the parameter  $\nu(x)$  and the corresponding distribution of the average frequency for a comparatively small value of the diffusion coefficient. The absence of imperfect cluster structures can be considered as a criterium of the absence of chaotic dynamics. Indeed, the regime of chaotic oscillations has not been registered in the performed numeric experiments. One can observe just quasi-periodic oscillations with different sets of independent frequencies. Characteristics of oscillations at the point  $x_1 = 25$  are presented in Fig. 10 in the regime of frequency clusters that are shown in Fig. 9(b) (for  $\alpha = 0.1$  and  $g = 0.01$ ). The spectrum and the ACF of  $a_1(x_1, t)$  oscillations, shown in Figs. 10(a) and 10(b) clearly indicate their regular

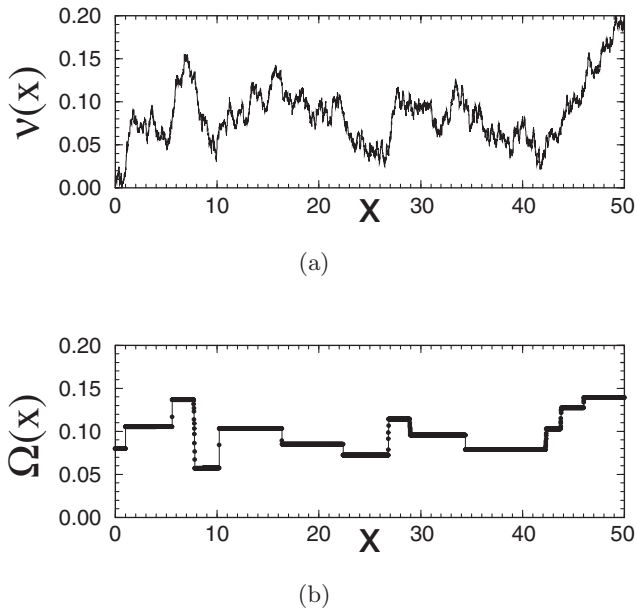


Fig. 9. (a) Random distribution of the parameter  $\nu(x)$  according to Eqs. (3) and (5) for  $\alpha = 0.1$  and  $\Delta = 0.2$  and (b) the corresponding distribution of the average frequency for the diffusion coefficient  $g = 0.01$ .

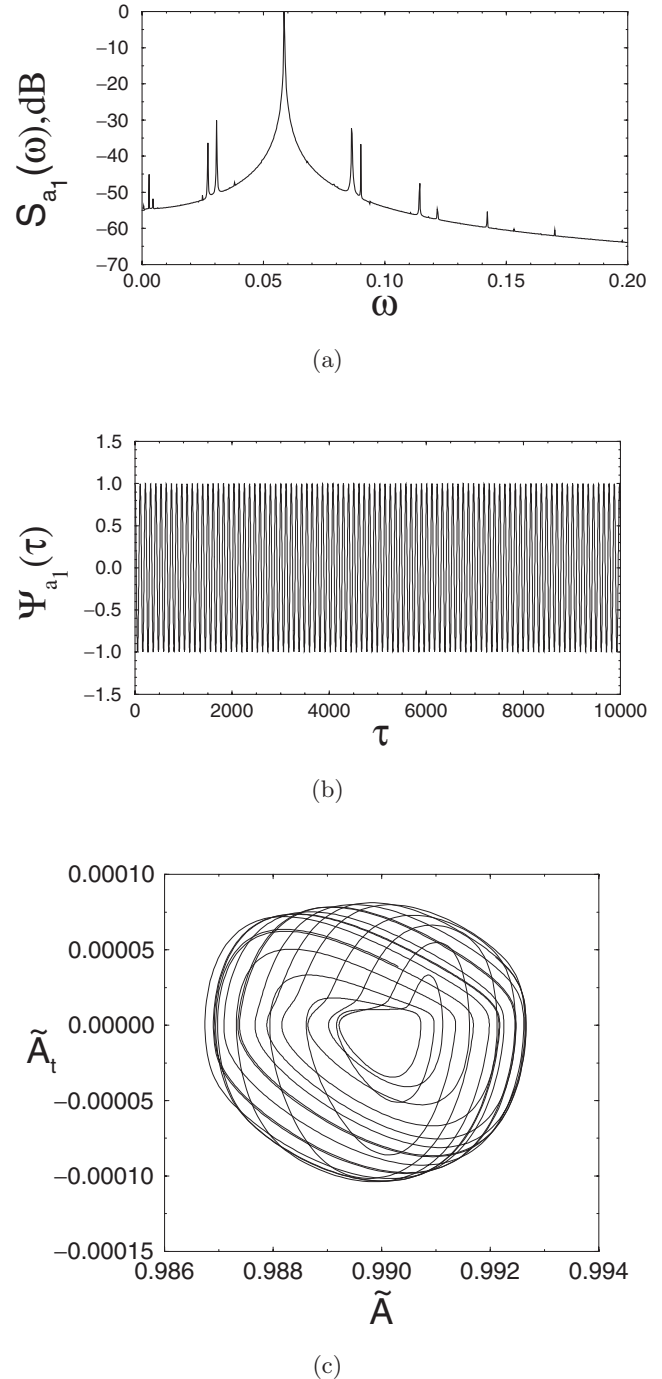


Fig. 10. Characteristics of oscillations at the point  $x_1 = 25$  for a random frequency mismatch along the special coordinate according to Eqs. (3) and (5) for  $\alpha = 0.1$ ,  $\Delta = 0.2$  and the diffusion coefficient  $g = 0.01$ . (a) Normalized power spectrum density of  $a_1(x_1, t)$  oscillations, (b) normalized ACF of  $a_1(x_1, t)$  oscillations, and (c) projection of oscillations on the plane  $(\tilde{A}(x_1, t), \tilde{A}_t(x_1, t))$ .

character. The form of the oscillation projection on the plane  $(\tilde{A}(x_1, t), \tilde{A}_t(x_1, t))$ , pictured in Fig. 10(c) enables one to conclude about the quasi-periodic character of the process  $a(x_1, t)$ .

## 7. Conclusion

The performed numerical studies enable us to make a number of important conclusions concerning dynamics of an inhomogeneous self-sustained oscillating medium. They are as follows:

- (i) Chaos and turbulence can be developed in a continuous self-sustained oscillating medium due to its inhomogeneity that can lead to a frequency mismatch at different points of the medium.
- (ii) Chaotic dynamics is observed if the inhomogeneity is determined by a linear dependence of a parameter on the spatial coordinate  $x$ . One may assume that the same condition can be applied to any function which “slowly changes” when varying  $x$ .
- (iii) A randomly defined inhomogeneity can simplify synchronization of medium elements and excludes the onset of chaotic dynamics.
- (iv) Temporal chaotic dynamics of the medium with linear inhomogeneity is uniquely related with the existence of a continuous monotone dependence of the average frequency of oscillations on the spatial coordinate, i.e. with the regime of imperfect frequency clusters.
- (v) From a viewpoint of spectral and correlation properties, chaotic oscillations within imperfect clusters qualitatively correspond to a model of harmonic noise. The rate of ACF decay is not defined by an exponential growth index of a perturbation but is connected with the instantaneous phase diffusion. Chaotic oscillations in intercluster regions possess a more complicated character, are characterized by a nonexponential decay of the ACF and cannot be compared with the model of harmonic noise.

## Acknowledgments

This work was partly supported by the BRHE Program (grant No. SR-006-X1), the RFBR (grant No. 04-02-16283a) and the INTAS (grant No. 01-2061). The authors express their gratitude to Dr. A. N. Pavlov and Prof. A. P. Chetverikov for their useful advice and help while working on this paper.

## References

- Afraimovich, V. S. & Shilnikov, L. P. [1983] “Strange attractors and quasiattractors,” in *Nonlinear Dynamics and Turbulence*, eds. Barenblatt, G. I., Iooss, G. &

- Joseph, D. D. (Pitman, Boston, London, Melbourne), pp. 1–34.
- Afraimovich, V. S., Nekorkin, V. I., Osipov, G. V. & Shalfeev, V. V. [1995] *Synchronization, Structures and Chaos in Nonlinear Synchronization Networks* (World Scientific, Singapore).
- Anishchenko, V. S., Aranson, I. S., Postnov, D. E. & Rabinovich, M. I. [1986] “Spatial synchronization and chaos development bifurcations in a chain of coupled self-sustained oscillators,” *Dokl. Akad. Nauk SSSR* **286**, 1120–1124 (in Russian).
- Anishchenko, V. S. [1995] *Dynamical Chaos — Models and Experiments* (World Scientific, Singapore).
- Anishchenko, V. S., Vadivasova, T. E., Okrokvertskhov, G. A., Kurths, J. & Strelkova, G. I. [2003] “Correlation analysis of dynamical chaos,” *Physica* **A325**, 199–212.
- Anishchenko, V. S., Vadivasova, T. E., Kurths, J., Okrokvertskhov, G. A. & Strelkova, G. I. [2004a] “Autocorrelation function and spectral linewidth of spiral chaos in a physical experiment,” *Phys. Rev.* **E69**, 036215(1–4).
- Anishchenko, V. S., Vadivasova, T. E. & Strelkova, G. I. [2004b] “Instantaneous phase method in studying chaotic and stochastic oscillations and its limitations,” *Fluct. Noise Lett.* **4**, L219–L229.
- Brandstater, A., Swift, J., Swinny, H. L. & Wolf, A. [1983] “Low-dimension chaos in a hydrodynamic system,” *Phys. Rev. Lett.* **5**, 1442–1445.
- Chaté, H. [1994] “Spatiotemporal intermittency regimes of the one-dimensional complex Ginzburg–Landau equation,” *Nonlinearity* **7**, 185–204.
- Diamant, N. E., Rose, P. K. & Davidson, E. J. [1970] “Computer simulation of intestinal slow-wave frequency gradient,” *Am. J. Physiol. — Legacy Content* **219**, 1684–1690.
- Ermentrout, G. B. & Kopell, N. [1984] “Frequency plateaus in a chain of weakly coupled oscillators,” *SIAM J. Math. Ann.* **15**, 215–237.
- Ermentrout, G. B. & Troy, W. C. [1986] “Phase locking in a reaction-diffusion system with a linear frequency gradient,” *SIAM J. Math. Ann.* **46**, 359–367.
- Gollub, J. P. & Benson, S. V. [1980] “Many routes to turbulent convection,” *J. Fluid Mech.* **100**, 449–470.
- Kuramoto, Y. [1984] *Chemical Oscillations, Waves and Turbulence*, Springer Series in Synergetics (Springer, Berlin).
- Linkens, D. A. & Satardina, S. [1977] “Frequency entrainment of coupled Hodgkin-Huxley — type oscillators for modeling gastro-intestinal electrical activity,” *IEEE Trans. Biomed. Engn.* **BME-24**, 362–365.
- Malreison, B., Atten, P., Bregé, P. & Dubois, M. [1983] “Dimension of strange attractors: An experimental determination for the chaos regime of two convective systems,” *J. Phys. Lett.* **44**, 897–902.

- Noak, B. R., Ohle, F. & Eckelman, H. [1991] "On cell formation in vortex streets," *J. Fluid Mech.* **227**, 293–308.
- Osipov, G. V., Pikovsky, A. S., Rosenblum, M. G. & Kurths, J. [1997] "Phase synchronization effects in a lattice of nonidentical Rössler oscillators," *Phys. Rev.* **E55**, 2353–2361.
- Osipov, G. V. & Sushchik, M. M. [1998] "Synchronized clusters and multistability in arrays of oscillators with different natural frequencies," *Phys. Rev.* **E58**, 7198–7207.
- Ruelle, D. & Takens, F. [1971] "On the nature of turbulence," *Commun. Math. Phys.* **20**, 167–192.
- Sakaguchi, H., Shinomoto, S. & Kuramoto, Y. [1978] "Local and global self-entrainments in oscillator lattices," *Progr. Theor. Phys.* **77**, 1005–1010.
- Sakaguchi, H. [1990] "Breakdown of the phase dynamics," *Progr. Theor. Phys.* **84**, 792–800.
- Sarna, S. K., Daniel, E. E. & Kingma, J. J. [1972] "Simulation of the electric — control activity of the stomach by an array of relaxation oscillators," *Digestive Diseases* **17**, 299–310.
- Shilnikov, L. P. [1997] "Mathematical problems of nonlinear dynamics: A tutorial," *Int. J. Bifurcation and Chaos* **7**, 1953–2001.
- Shraiman, B. I., Pumir, A., Van Saarloos, W., Hohenberg, P. C., Chaté, H. & Holen, M. [1992] "Spatiotemporal chaos in the one-dimensional complex Ginzburg–Landau equation," *Physica* **D57**, 241–248.
- Strogatz, S. H. & Mirollo, R. E. [1988] "Phase-locking and critical phenomena in lattices of coupled nonlinear oscillators with random intrinsic frequencies," *Physica* **D31**, 143–168.
- Swinney, H. L., Fenstermocher, P. B. & Gollub, J. P. [1977] "Transition to turbulence in a fluid flow," *Sinergetics*, ed. Haken, Y. (Springer, Berlin), pp. 60–65.
- Vadivasova, T. E., Strelkova, G. I. & Anishchenko, V. S. [2001] "Phase-frequency synchronization in a chain of periodic oscillators in the presence of noise and harmonic forcings," *Phys. Rev.* **E63**, 036225.
- Winfree, A. T. [1980] *The Geometry of Biological Time* (Springer, NY).
- Wolf, A., Swift, J. B., Swinney, H. L. & Vastano, J. A. [1985] "Determining Lyapunov exponents from a time series," *Physica* **D16**, 285–317.
- Yamaguchi, Y. & Shimizu, H. [1984] "Theory of self-synchronization in the presence of native frequency distribution and external noises," *Physica* **D11**, 212–226.